the FEBS Journal

Motion of the Ca^{2+}-pump captured

Masatoshi Yokokawa[1,2] and Kunio Takeyasu[1]

1 Kyoto University Graduate School of Biostudies, Japan
2 Graduate School of Pure and Applied Science, University of Tsukuba, Japan

Keywords
atomic force microscopy; ion pump; P-type ATPase; SERCA; single molecular reaction analysis

Correspondence
M. Yokokawa, Graduate School of Pure and Applied Science, University of Tsukuba, 1-1-1 Tennoudai, Tsukuba 305-8573, Japan
Fax: +81 29 853 4490
Tel: +81 29 853 5600 (5466)
E-mail: yokokawa@ims.tsukuba.ac.jp

(Received 9 March 2011, revised 24 May 2011, accepted 16 June 2011)

doi:10.1111/j.1742-4658.2011.08222.x

Studies of ion pumps, such as ATP synthetase and Ca^{2+}-ATPase, have a long history. The crystal structures of several kinds of ion pump have been resolved, and provide static pictures of mechanisms of ion transport. In this study, using fast-scanning atomic force microscopy, we have visualized conformational changes in the sarcoplasmic reticulum Ca^{2+}-ATPase (SERCA) in real time at the single-molecule level. The analyses of individual SERCA molecules in the presence of both ATP and free Ca^{2+} revealed up–down structural changes corresponding to the Albers–Post scheme. This fluctuation was strongly affected by the ATP and Ca^{2+} concentrations, and was prevented by an inhibitor, thapsigargin. Interestingly, at a physiological ATP concentrations, the up–down motion disappeared completely. These results indicate that SERCA does not transit through the shortest structure, and has a catalytic pathway different from the ordinary Albers–Post scheme under physiological conditions.

Introduction

Skeletal muscle contraction is subject to actin-linked regulation by troponins [1,2]. The physiological player in its molecular mechanism is Ca^{2+}, which is released into the cytoplasm from the sarcoplasmic reticulum (SR) through the Ca^{2+}-release channel. This removes the troponin inhibition of the actin–myosin interaction, and induces muscle contraction. When the muscle relaxes, Ca^{2+} needs to be removed from the cytoplasm by the Ca^{2+}-pump (Ca^{2+}-ATPase) [3,4], which accumulates Ca^{2+} inside the SR against its concentration gradient. The importance of the SR Ca^{2+}-pump was realized in the early 1960s by Ebashi and Lipmann [5,6] and, since then, most of the molecular components in the regulation of skeletal muscle contraction have been identified, crystallized, and have their genes cloned [1,2,7]. In this study, the motion of the Ca^{2+}-pump (sarco-endoplasmic reticulum Ca^{2+}-ATPase 1a, SERCA) in the rabbit SR membrane was captured by using fast-scanning atomic force microscopy (FSAFM) [8–10].

Results and Discussion

Up–down motion of SERCA

Purified SR vesicles containing SERCA were directly immobilized on a mica surface through electrostatic force without any modification or chemical treatment (solid supported membrane [11,12]). It appears that the vesicles (the diameters of which vary from several tens to hundreds of nanometers) can be adsorbed on the mica surface without being broken, resulting in 'double membranes', and these flatten on the mica surface with a thickness of $\sim$ 10 nm. Unfortunately, the smallness of the vesicles and their loose adhesion to the mica surface make FSAFM observation difficult.

Abbreviations
AFM, atomic force microscopy; DOC, deoxycholate; FSAFM, fast-scanning atomic force microscopy; SD, standard deviation; SERCA, sarco-endoplasmic reticulum Ca^{2+}-ATPase; SR, sarcoplasmic reticulum; TG, thapsigargin.

On the other hand, after treatment with deoxycholate (DOC), a detergent that is frequently used to solubilize and further purify SERCA for crystallization [13,14], some SR membranes fused with each other and were adsorbed onto the mica surface as lipid bilayer membranes with a thickness of 5.1 ± 0.6 nm [mean ± standard deviation (SD), $N = 23$]. These DOC-treated SR membranes immobilized on the mica surface contained well-separated SERCA, the density of which was less than a few SERCA molecules per μm^2, owing to the partial formation of 2D crystals. These were used for FSAFM analysis. The quality of the membranes was always ensured by SDS/PAGE, atomic force microscopy (AFM), and immunofluorescence microscopy (Fig. S1A,B, Doc. S1).

The immobilization force in our specimen was strong enough to minimize the random diffusion of SERCA molecules, resulting in an averaged 2D diffusion coefficient of 0.4 ± 0.2 $nm^2 \cdot s^{-1}$ (mean ± SD). Thus, SERCA molecules keep the same position during single line scanning [8,15] by FSAFM. This means that the previously demonstrated single line scanning (2D) observation technique, which has much higher time resolution than the normal (3D) observation technique, is available for short-duration (< 1 s) observation. However, this immobilization force did not interfere with the flexible conformational changes of SERCA molecules in the membrane on the mica surface (for details, see below).

In a buffer solution containing both 10 nM ATP and 100 μM free Ca^{2+}, FSAFM captured the motion of the SERCA molecule (purple dot) embedded in the single lipid bilayer on mica (Fig. 1A, Movie S1). Up–down motions and shape changes between taller (compacted) and shorter (open and Y-shaped) forms of SERCA molecules were clearly evident. The most straightforward interpretation of these results is that the height fluctuation and shape changes correspond to the conformational changes (long-distance movement of the N-domain and rotational motion of the A-domain) of SERCA during the ATP-mediated ion transport reaction [14,16–19].

The single line scanning method [8,15], in which an AFM probe repeatedly scanned on a single line (along the *y*-axis direction in Fig. 1B) at a rate of 250–1000 Hz, provided a higher time resolution than the normal (3D) observation technique (a few frames per second), and the rapid up–down conformational changes of SERCAs were repeatedly observed as sharp peaks (Fig. 1B, black arrowhead). The short-lived elevated state of SERCA was 2.3 ± 0.4 nm (mean ± SD, $N = 65$) taller than the other states. This elevation value is very similar to the height difference between the $E1Ca^{2+}$ form [14], in which the N-domain is widely separated from the A-domain and P-domain, and the other compacted forms of SERCA (E1ATP, E1P, E2P, and E2) estimated from 3D structural models [14,16–18]. To test this suggestion, the heights of the $E1Ca^{2+}$ form (shorter structure) and the E2 form (one of the taller structures) were measured. In the buffer solution containing 100 μM free Ca^{2+} (with an EGTA-Ca^{2+} buffering system; see Experimental procedures) without any nucleotide, it was expected that most SERCA would remain as the ATP-unbound and Ca^{2+}-bound $E1Ca^{2+}$ form. In the histogram (Fig. 2A) of the distribution of the height of the projection of the embedded molecule above the flat membrane surface, the average height was 5.4 ± 0.8 nm, which is in good agreement with the height of the cytoplasmic domain estimated from the X-ray crystallography data of the $E1Ca^{2+}$ form [14]. In the buffer solution containing 10 nM free Ca^{2+} without any nucleotide (Fig. 2B), the addition of 10 μM thapsigargin (TG), which fixes the enzyme in a form analogous to E2 [16,20,21], shifted the averaged height to a higher value. The histogram of the height difference after incubation with TG clearly illustrated two peaks near 5.4 ± 0.7 nm and 7.2 ± 1.0 nm (Fig. 2C). The mean value of the taller peak (7.2 nm) corresponds well to the height of the cytoplasmic domain of SERCA in the E2 state [16]. Although we used purified proteins, some deformed protein (< 40%), resulting from the sample preparation procedure or FSAFM scanning, could be contained. Therefore, some SERCAs that do not undergo conformational changes at all over the period of observation in the presence of both ATP and Ca^{2+} were excluded from the following analyses.

Visual characteristics of the Albers–Post scheme

The number of peaks (i.e. the number of up–down conformational changes of SERCA) per unit time was dependent on the ATP concentration (Fig. 1B,C). The number of peaks within 1 s was counted in the presence of 100 μM free Ca^{2+} and various concentrations (0–100 μM) of ATP, and the data are plotted in Fig. 3A. The graph shows a clear dependence on ATP concentration, although only the frequencies at medium (1 μM), extremely high and low ATP concentrations are shown, owing to limitations in experimental accuracy. The maximum number of conformational changes of SERCA seen under our experimental conditions was about 50 s^{-1}. These height fluctuations were only observed in the presence of both ATP and Ca^{2+}, and the motion was strongly inhibited by

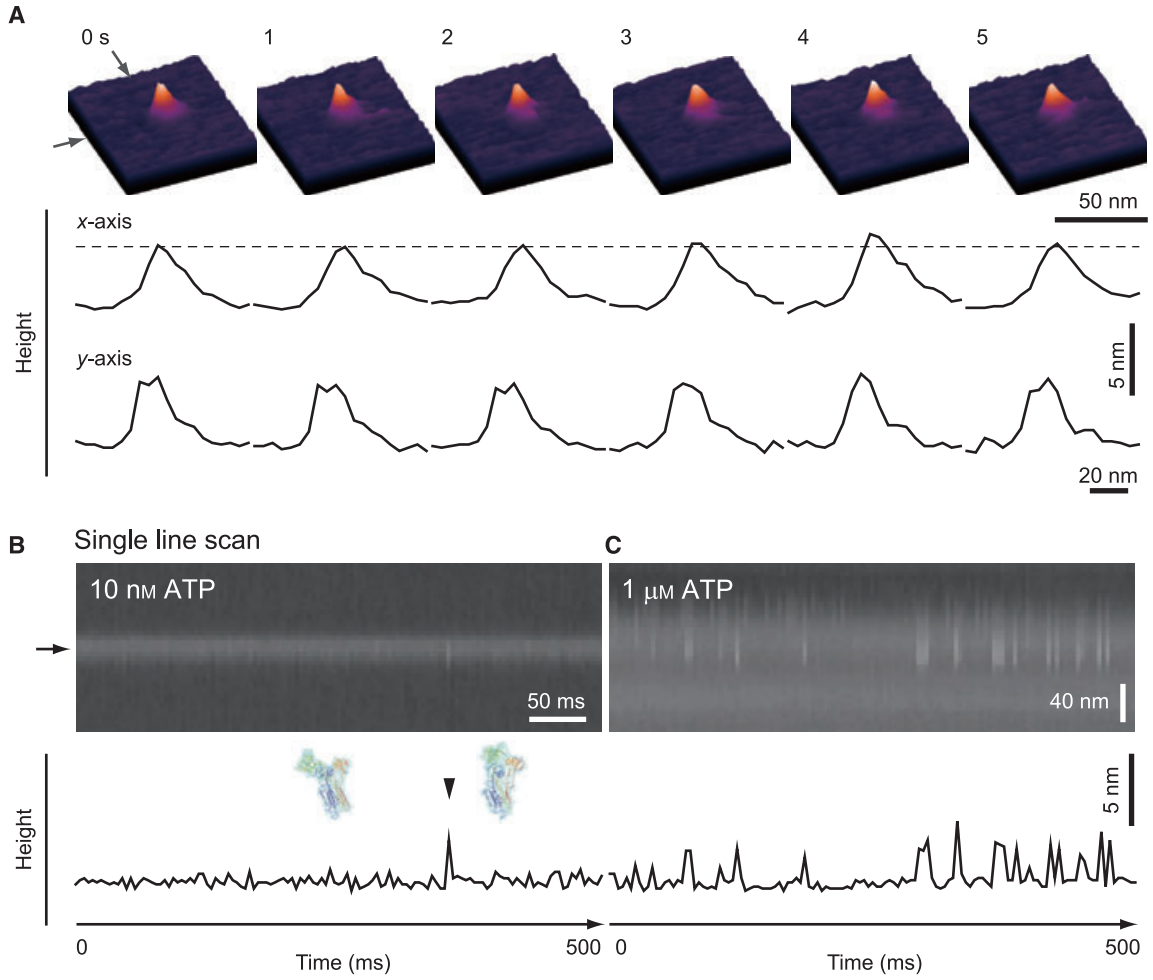

Fig. 1. Single-molecule imaging of SERCA dynamics in the presence of nucleotide and Ca^{2+}. (A) Time-lapse sequence FSAFM images of SERCA in the SR membrane on a mica surface in a buffer solution were obtained in the presence of 10 nM ATP and 100 μM free Ca^{2+} with 192 × 144 pixels at a rate of one frame per second. The images (40 × 40 pixels) presented here were selected from the original data without any modification. Scale bars: 20 nm. The *z*-scale is 20 nm. The resulting profiles are shown in the corresponding lower panel. The broken line indicates a height of 5.5 nm from the membrane surface. (B, C) Single line scan (2D observation) FSAFM images of SERCA were obtained in the presence of 100 μM free Ca^{2+} and in the presence of 10 nM (B) and 1 μM ATP (C), respectively [scanning rate of 250 Hz, scan scale of 208 nm (*y*-axis direction in the FSAFM images), and *z*-scale of 40.0 nm]. In these FSAFM images, individual SERCA molecules can be seen as tubular features. The lower panels show the *x*-axis cross-sections positioned at the line indicated by the arrow beside the FSAFM images, which represent typical height fluctuations under the conditions used. The *x*-axis is time and the *y*-axis is the height of SERCA. SERCA structures 2–3 nm taller (elevated conformations) and height fluctuations can be seen as the bright (white) sharp signals. These up–down conformational changes of SERCA were repeatedly observed.

addition of TG to the buffer solution. Considering the crystallography data and the fact that, under normal buffer conditions, the SERCA reaction usually goes in one direction (catalytic direction) in the Albers–Post scheme (Fig. S1C) [4,22,23], one peak corresponds to one catalytic cycle (Ca^{2+}-binding shorter conformation → ATP hydrolysis-mediated elevated conformations → Ca^{2+}-binding shorter conformation), and the number of peaks must correspond to the velocity of the catalytic cycle of SERCA. Interestingly, the turnover rate, ATP concentration dependency and TG inhibition of up–down motion are quite similar to those of ATPase activity and Ca^{2+} uptake reported previously [24,25]; for example, a conventional biochemical assay showed that the turnover rate of ATP hydrolysis of SERCA linearly increased with ATP concentrations of ~ 1 μM [26].

The lifetime of the elevated conformation (i.e. peak width) in the presence of both ATP and Ca^{2+} was measured in the single line FSAFM images, and

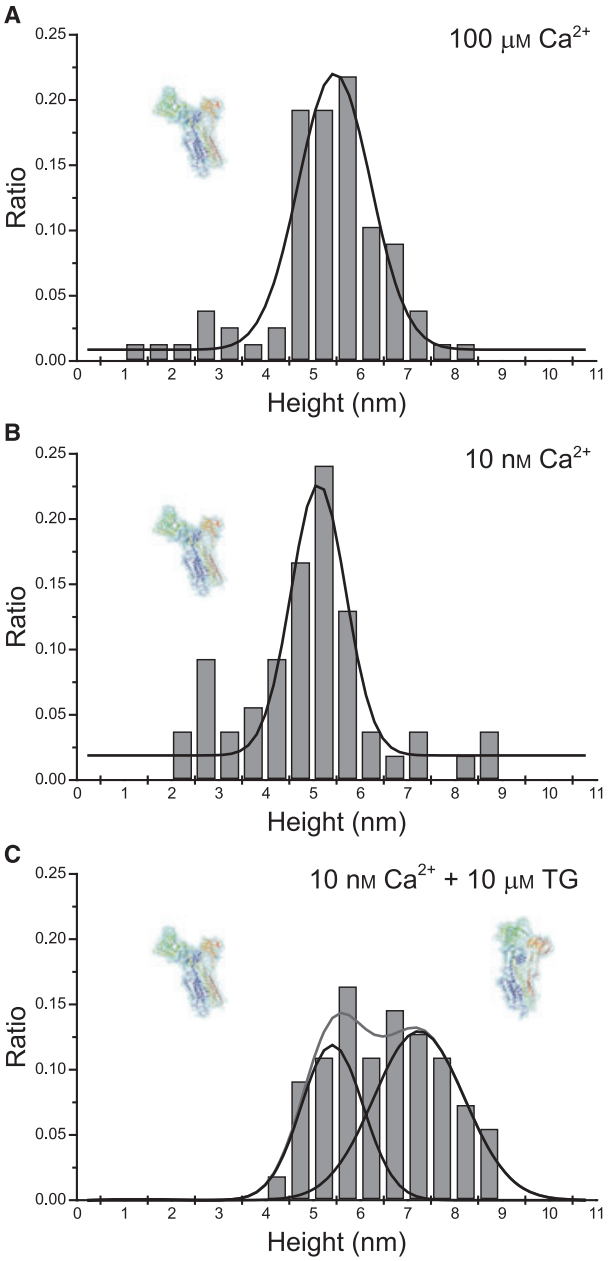

Fig. 2. Histograms of the height differences between the top of SERCA and the surface of the membrane. Statistical section analyses of SERCA were performed with the data obtained in the presence of (A) 100 μM free Ca^{2+} (N = 78), (B) 10 nM free Ca^{2+} (N = 54), (C) 10 nM free Ca^{2+} and 10 μM TG, after 30 min incubation (N = 82). The lines are Gaussian fits of the height difference data.

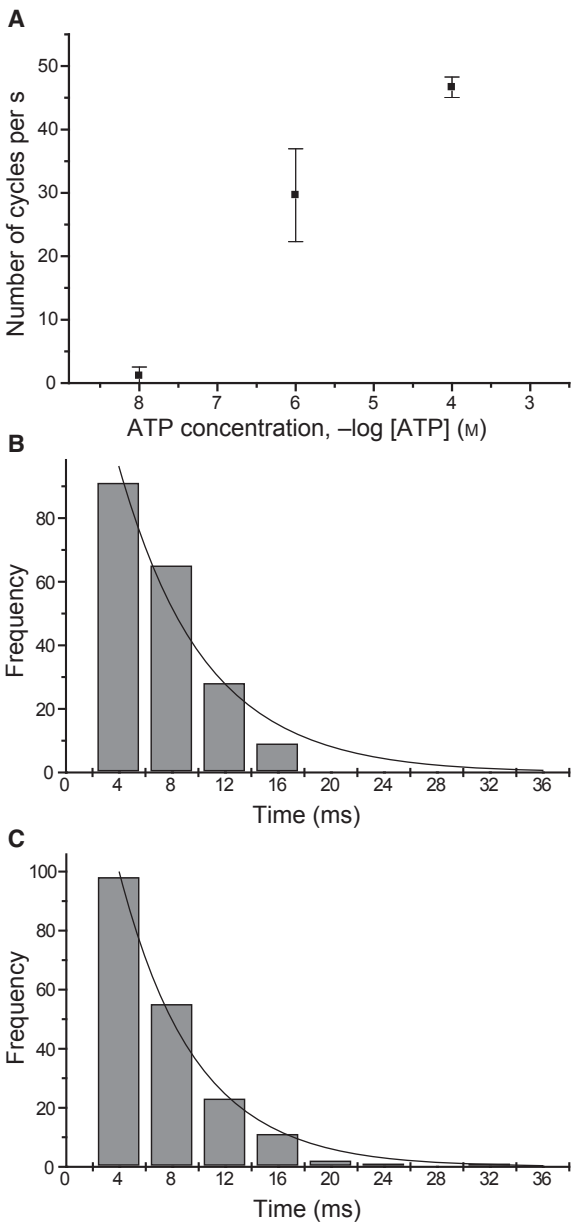

Fig. 3. ATP concentration dependence of the SERCA reaction. (A) Number of peaks per second with 100 μM free Ca^{2+} and increasing ATP concentrations in the range 10 nM to 100 μM. (B, C) Typical distributions of the lifetime of the elevated conformations of SERCA in the presence of 100 μM free Ca^{2+} and 10 nM (B) and 100 μM ATP (C). The histograms were fitted with a single-exponential function by using the following equation: $F(t) = C_1 k_1 \exp(-k_1 t)$, where $F(t)$ is the number of elevated conformation C_1 is the number of the total events, and k_1 is the rate constant. The rate constants (k_1) were obtained by the nonlinear least-square curve-fitting method.

plotted as a histogram (Fig. 3B,C). The histogram was simply fitted to a single-exponential model to obtain the rate constant of the nucleotide-induced conformational change: $F(t) = C_1 k_1 \exp(-k_1 t)$, where $F(t)$ is the number of elevated conformation with a lifetime t, C_1 is the number of the total events, and k_1 is the rate constant. The obtained rate constants (k_1) were 0.15 ms^{-1} at 10 nM ATP and 0.17 ms^{-1} at 100 μM

ATP, respectively. The rate constant did not depend on the nucleotide concentration in the range from 10 nM to 100 μM, indicating that the up–down conformational change of SERCA (i.e. the reaction after ATP binding) did not require further ATP binding or hydrolysis, and that once a single ATP hydrolysis reaction started, it was not affected by additional ATP.

The time courses of height fluctuation in the presence of a much lower free Ca^{2+} concentration and various ATP concentrations are summarized in Fig. 4A. The data clearly show that a sharp peak (quick up–down conformational change of SERCA) was rarely observed and that the lifetime of the elevated conformation was apparently increased. The increased lifetime of the elevated conformation at low Ca^{2+} concentration could reasonably be a reflection of lowered ATPase activity at low Ca^{2+} concentrations [25]. Thus, the conformational change from the elevated conformation to the shorter conformation was dependent on Ca^{2+} concentration. This means that the transition from elevated to shorter conformations represented the Ca^{2+}-binding-step, the E1 $\rightarrow$ E1Ca^{2+} transition, and that the E1 state, which has not been crystallized, also has an elevated structure. The elongation time of the elevated state at a low free Ca^{2+} concentration easily explains the Ca^{2+} concentration dependency of the ATPase activity measured by biochemical experiments [25].

SERCA dynamics under physiological conditions

In a buffer solution containing both 1.0 mM ATP and 100 μM free Ca^{2+}, approximating physiological ATP conditions, SERCA molecules maintained elevated structures for a long time without up–down motions, even though the time resolution of FSAFM measurement was increased up to 1000 kHz (Fig. 4B). We note that the AFM probe stayed on the SERCA for only 50 μs during a single line scan, indicating that our experimental method can potentially detect short-lived shorter structures with a time resolution of 50 μs. If the Albers–Post scheme reaction mechanism can be applied at higher ATP concentrations, the time between peaks should be shortened. Actually, this was true in our experiments up to several 100 μM. However, it is also notable that, at much higher ATP concentrations, we could not detect the shorter form at all with a time resolution of 50 μs. This fact suggests two possibilities: one is that the lifetime of the smaller form is < 50 μs; another is that SERCA does not have a shorter form under these conditions. As the conformational change from shorter to elevated structures is induced by binding of ATP, such a diffusion process will not be so fast. Furthermore, assuming that the lifetime of the shorter form is < 50 μs, it becomes difficult to understand ATPase activity at an even higher ATP condition (above 1 mM) [24]. It is due to the lifetime of the elevated conformation being independent of ATP concentration and the average lifetime was in the order of ms (Figure 3B,C). Therefore, we propose that SERCA does not have the shorter (E1Ca^{2+}) form at higher ATP concentrations.

In conclusion, at physiological ATP concentrations (of the millimolar order), SERCA does not transit the E1Ca^{2+} state [14], in which SERCA has the shortest structure, and has a catalytic pathway different from the ordinary Albers–Post scheme. This hypothesis is further supported by previous X-ray crystallographic

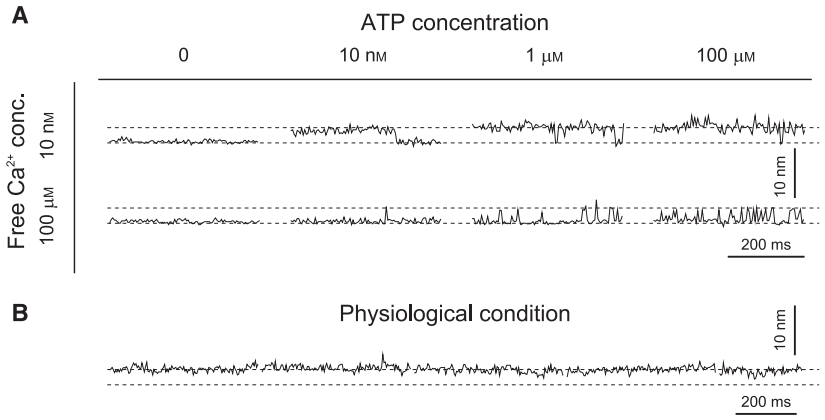

Fig. 4. Typical single line scan data obtained with buffer conditions. (A) Representative single line scan graphs obtained at increasing ATP concentration in the range 0–100 μM and in the presence of 10 nM and 100 μM free Ca^{2+}. (B) Sequential single line scan graphs (which correspond to an observation period of ~ 2 s) in the presence of both 1 mM ATP and 100 μM free Ca^{2+}. The broken lines indicate heights of 5.5 nm and 8.0 nm from the membrane surface.

studies [27,28], in which the E2P*-ATP, E2-ATP and Ca2E1–P-ADP structures were crystallized; SERCA assumes its compact structure during the whole reaction cycle under physiological conditions. It is also notable that many biochemical experiments have shown that ATP exhibits an additional stimulatory effect on the reaction cycle at higher ATP concentrations (> 100 μM) [24], like the Na^+/K^+-ATPase [29–31].

Experimental procedures

Materials

All chemicals used in these experiments were of reagent grade. SR was purified and washed with DOC as described previously [13,14]. The purified SR and DOC-washed SR were stored in liquid nitrogen. The protein concentration in SR was determined with the Bradford protein assay (Bio-Rad, Hercules, CA, USA) calibrated by quantitative amino acid analysis. Before use, the stock SR (or DOC-washed SR) solution was diluted (50 $\mu g \cdot mL^{-1}$ for SERCA in 75 mM Mops/KOH, 150 mM KCl, 7.5 mM $MgCl_2$, 0.6 mM $CaCl_2$ and 0.5 mM EGTA, pH 7.0).

FSAFM observation

Our FSAFM system was developed on the basis of the system described by Ando *et al*. [10]. Details are given in our previous paper [8]. We used newly developed piezo scanners, the resonance frequencies of which are *xy* 30 kHz and *z* 600 kHz. Small silicon nitride cantilevers were used (BL-AC7EGS-A2 cantilevers; Olympus, Tokyo, Japan). Their resonant frequencies in water were ~ 600 kHz, and the spring constants in water were ~ 0.1–0.2 $N \cdot m^{-1}$. Each cantilever had an electron beam deposited probe. The temperature around the scanning area on the sample surface was estimated to be ~ 40 °C.

A 3 μL droplet of diluted SR (or DOC-washed SR) solution was directly applied onto the surface of freshly cleaved mica (the diameter is 1.0 mm). After incubation for 30 min at room temperature, the sample was gently washed several times with the buffer to remove unadsorbed SR and kept in the same buffer solution until used. FSAFM imaging in tapping mode was performed in the same buffer solution with or without ATP, $CaCl_2$, and TG (the final concentration of TG was 10 μM). The various $CaCl_2$ concentrations used to obtain the required free Ca^{2+} concentrations were calculated with MAXC HELATOR (http://maxchelator.stanford.edu), using the dissociation constants therein [32].

All FSAFM images were obtained with a scanning speed of typically one to five frames per second for 3D observation and 250 Hz or 1000 Hz (lines per second) for 2D observation. Movie (images) analysis was performed with IMAGEJ (http://rsbweb.nih.gov/ij/).

Acknowledgements

We thank C. Toyoshima for kindly supplying the purified SR used in our experiments. We also thank H. Suzuki and members of OLYMPUS Corporation for helpful discussion and much technical advice. This work was supported by grants from SENTAN, JST to K. Takeyasu and a Grant-in-Aid for Scientific Research in Priority Areas 'Protein community' (no. 20059018) of the Ministry of Education, Culture, Sports, Science and Technology, Japan to M. Yokokawa.

References

1 Berchtold MW, Brinkmeier H & Muntener M (2000) Calcium ion in skeletal muscle: its crucial role for muscle function, plasticity, and disease. *Physiol Rev* **80**, 1215–1265.
2 Ohtsuki I & Morimoto S (2008) Troponin: regulatory function and disorders. *Biochem Biophys Res Commun* **369**, 62–73.
3 Hasselbach W & Makinose M (1961) The calcium pump of the 'relaxing granules' of muscle and its dependence on ATP-splitting. *Biochem Z* **333**, 518–528.
4 Kuhlbrandt W (2004) Biology, structure and mechanism of P-type ATPases. *Nat Rev Mol Cell Biol* **5**, 282–295.
5 Ebashi S (1963) Third component participating in the superprecipitation of 'natural actomyosin'. *Nature* **200**, 1010.
6 Ebashi S & Lipmann F (1962) Adenosine triphosphate-linked concentration of calcium ions in a particulate fraction of rabbit muscle. *J Cell Biol* **14**, 389–400.
7 Ebashi S & Kodama A (1965) A new protein factor promoting aggregation of tropomyosin. *J Biochem* **58**, 107–108.
8 Yokokawa M, Wada C, Ando T, Sakai N, Yagi A, Yoshimura SH & Takeyasu K (2006) Fast-scanning atomic force microscopy reveals the ATP/ADP-dependent conformational changes of GroEL. *EMBO J* **25**, 4567–4576.
9 Crampton N, Yokokawa M, Dryden DT, Edwardson JM, Rao DN, Takeyasu K, Yoshimura SH & Henderson RM (2007) Fast-scan atomic force microscopy reveals that the type III restriction enzyme EcoP15I is capable of DNA translocation and looping. *Proc Natl Acad Sci USA* **104**, 12755–12760.
10 Ando T, Kodera N, Takai E, Maruyama D, Saito K & Toda A (2001) A high-speed atomic force microscope for studying biological macromolecules. *Proc Natl Acad Sci USA* **98**, 12468–12472.
11 Tanaka M & Sackmann E (2005) Polymer-supported membranes as models of the cell surface. *Nature* **437**, 656–663.

12 Tadini Buoninsegni F, Bartolommei G, Moncelli MR, Inesi G & Guidelli R (2004) Time-resolved charge translocation by sarcoplasmic reticulum Ca-ATPase measured on a solid supported membrane. *Biophys J* **86**, 3671–3686.
13 Stokes DL & Green NM (1990) Three-dimensional crystals of CaATPase from sarcoplasmic reticulum. Symmetry and molecular packing. *Biophys J* **57**, 1–14.
14 Toyoshima C, Nakasako M, Nomura H & Ogawa H (2000) Crystal structure of the calcium pump of sarcoplasmic reticulum at 2.6 A resolution. *Nature* **405**, 647–655.
15 Viani MB, Pietrasanta LI, Thompson JB, Chand A, Gebeshuber IC, Kindt JH, Richter M, Hansma HG & Hansma PK (2000) Probing protein–protein interactions in real time. *Nat Struct Biol* **7**, 644–647.
16 Toyoshima C & Nomura H (2002) Structural changes in the calcium pump accompanying the dissociation of calcium. *Nature* **418**, 605–611.
17 Toyoshima C & Mizutani T (2004) Crystal structure of the calcium pump with a bound ATP analogue. *Nature* **430**, 529–535.
18 Toyoshima C, Nomura H & Tsuda T (2004) Lumenal gating mechanism revealed in calcium pump crystal structures with phosphate analogues. *Nature* **432**, 361–368.
19 Sorensen TL, Moller JV & Nissen P (2004) Phosphoryl transfer and calcium ion occlusion in the calcium pump. *Science* **304**, 1672–1675.
20 Inesi G & Sagara Y (1992) Thapsigargin, a high affinity and global inhibitor of intracellular Ca^{2+} transport ATPases. *Arch Biochem Biophys* **298**, 313–317.
21 Sagara Y & Inesi G (1991) Inhibition of the sarcoplasmic reticulum Ca^{2+} transport ATPase by thapsigargin at subnanomolar concentrations. *J Biol Chem* **266**, 13503–13506.
22 Moller JV, Juul B & le Maire M (1996) Structural organization, ion transport, and energy transduction of P-type ATPases. *Biochim Biophys Acta* **1286**, 1–51.
23 de Meis L & Vianna AL (1979) Energy interconversion by the Ca^{2+}-dependent ATPase of the sarcoplasmic reticulum. *Annu Rev Biochem* **48**, 275–292.
24 Verjovski-Almeida S & Inesi G (1979) Fast-kinetic evidence for an activating effect of ATP on the Ca^{2+} transport of sarcoplasmic reticulum ATPase. *J Biol Chem* **254**, 18–21.
25 Dode L, Vilsen B, Van Baelen K, Wuytack F, Clausen JD & Andersen JP (2002) Dissection of the functional differences between sarco(endo)plasmic reticulum Ca^{2+}-ATPase (SERCA) 1 and 3 isoforms by steady-state and transient kinetic analyses. *J Biol Chem* **277**, 45579–45591.
26 Dode L, Andersen JP, Raeymaekers L, Missiaen L, Vilsen B & Wuytack F (2005) Functional comparison between secretory pathway Ca^{2+}/Mn^{2+}-ATPase (SPCA) 1 and sarcoplasmic reticulum Ca^{2+}-ATPase (SERCA) 1 isoforms by steady-state and transient kinetic analyses. *J Biol Chem* **280**, 39124–39134.
27 Olesen C, Picard M, Winther AM, Gyrup C, Morth JP, Oxvig C, Moller JV & Nissen P (2007) The structural basis of calcium transport by the calcium pump. *Nature* **450**, 1036–1042.
28 Jensen AM, Sorensen TL, Olesen C, Moller JV & Nissen P (2006) Modulatory and catalytic modes of ATP binding by the calcium pump. *EMBO J* **25**, 2305–2314.
29 Post RL, Hegyvary C & Kume S (1972) Activation by adenosine triphosphate in the phosphorylation kinetics of sodium and potassium ion transport adenosine triphosphatase. *J Biol Chem* **247**, 6530–6540.
30 Clausen JD, McIntosh DB, Anthonisen AN, Woolley DG, Vilsen B & Andersen JP (2007) ATP-binding modes and functionally important interdomain bonds of sarcoplasmic reticulum Ca^{2+}-ATPase revealed by mutation of glycine 438, glutamate 439, and arginine 678. *J Biol Chem* **282**, 20686–20697.
31 Yamamoto T & Tonomura Y (1967) Reaction mechanism of the Ca^{++}-dependent ATPase of sarcoplasmic reticulum from skeletal muscle. I. Kinetic studies. *J Biochem* **62**, 558–575.
32 Bers DM, Patton CW & Nuccitelli R (1994) A practical guide to the preparation of Ca^{2+} buffers. *Methods Cell Biol* **40**, 3–29.

Supporting information

The following supplementary material is available:
Doc. S1. Supplementary materials and methods.
Fig. S1. Quality of intact SR and DOC-washed SR.
Movie S1. Single-molecule imaging of the SERCA dynamics in the presence of nucleotide and calcium ions.

This supplementary material can be found in the online version of this article.

Please note: As a service to our authors and readers, this journal provides supporting information supplied by the authors. Such materials are peer-reviewed and may be re-organized for online delivery, but are not copy-edited or typeset. Technical support issues arising from supporting information (other than missing files) should be addressed to the authors.